

Zirconium Phosphate as a Performance Booster for Direct Methanol Fuel Cells

Carlos E. Mendesa, Ahmed S. Al-Farsib, Layla H. Mansoorc, Fatima Benalid, and Khalid A. Rashide

a Department of Mechanical and Mechatronics Engineering, University of São Paulo, Av. Prof. Luciano Gualberto, 380, São Paulo 05508-010, Brazil

b King Fahd University of Petroleum & Minerals, The Graduate School of Natural and Applied Sciences, Mechanical Engineering Department, Dhahran 31261, Saudi Arabia

c American University of Beirut, Department of Polymer Science and Technology, Riad El-Solh, Beirut 1107 2020, Lebanon

d Cadi Ayyad University, Department of Energy Systems Engineering, Avenue Abdelkarim Elkhattabi, Marrakesh 40000, Morocco

e Khalifa University, Faculty of Engineering, Abu Dhabi, UAE

Abstract

Nafion/zirconium hydrogen phosphate (ZrP) composite membranes containing 2.5 wt.% ZrP (NZ-2.5) or 5 wt.% ZrP (NZ-5) were prepared to improve the performance of a direct methanol fuel cell (DMFC). The influence of ZrP content on the Nafion matrix is assessed through characterization techniques, such as Thermogravimetric Analysis (TGA), X-ray Diffraction (XRD), Scanning Electron Microscopy (SEM), Electrochemical Impedance Spectroscopy (EIS), and water uptake measurement. Performance testing of the DMFCs based on these composite membranes as well as commercial Nafion® 115 membranes were performed using a computer aided fuel cell test station for different values of cell temperature (40°C, 60°C, 80°C, and 100°C) and methanol concentration (0.75 M, 1.00 M, and 1.50 M). Characterization studies indicated that incorporation of ZrP into polymer matrix enhanced the water uptake and proton conductivity values of Nafion membrane. The results of the performance tests showed that the Membrane Electrode Assembly (MEA) having NZ-2.5 provided the highest performance with the peak power density of 551.52 W/m² at 100°C and 1.00 M. Then, the performances of the MEAs having the same NZ-2.5 membrane but different cathode catalysts were investigated by fabricating two different MEAs using cathode catalysts made of Pt/C-ZrP and Pt/C (HiSPEC® 9100). According to the results of these experiments, the MEA having NZ-2.5 membrane and Pt/C (HiSPEC® 9100) cathode catalyst containing 10 wt.% of ZrP exhibited the highest performance with the peak power density of 620.88 W/m² at 100°C and 1.00 M. In addition, short-term stability tests were conducted for all the MEAs. The result of the stability tests revealed that introduction of ZrP to commercial (HiSPEC® 9100) cathode catalyst improves its stability characteristics.

Keywords: Direct methanol fuel cell, Nafion/ZrP composite membrane, Zirconium hydrogen phosphate, Membrane electrode assembly, Stability

1. Introduction

Direct methanol fuel cell (DMFC) is one of the emerging technologies that could be used specifically in portable applications due to its advantages, such as easy storage, high energy density, and low cost of methanol, low emissions, and direct oxidation of methanol without the need of a reformer [1-3]. However, there are still some challenges towards the wide usage of this technology in commercial products due to their low performance mainly because of the sluggish methanol oxidation kinetics at the anode, methanol crossover through the membrane, and high cost as it is made of precious electrocatalysts. To overcome these challenges, there has been an active ongoing research done by many research institutes that includes the development and testing of DMFCs with different materials and manufacturing techniques (e.g., [4-6]). The main focus on these research activities is the development of high performance and durable Membrane Electrode Assembly (MEA).

One of the important components of MEA is the membrane, which acts as an electrolyte to carry the protons from the anode to cathode. The membrane also creates a barrier by preventing the transport of electrons from one electrode to the other [7]. Conventionally, DuPont's Nafion[®] 117, 115 or 212 has been used as the membrane for this type of fuel cell due to its chemical features, such as high proton conductivity and chemical stability at relatively low operating temperatures (up to 80°C). The proton conduction mechanism through this membrane depends markedly on the movement of protons with the help of sulfonic acid (SO₃H) groups as long as water exists. The membrane therefore should be well-hydrated to maintain an appropriate hydration level [8]. Although Nafion[®] membranes provide these aforementioned desirable properties at low operating temperatures (<80°C), as the temperature becomes higher than 80°C, the membrane starts to dehydrate and becomes less effective in reference to proton conductivity [9]. As a result of this dehydration problem, the performance of DMFC deteriorates due mainly to decrease in the proton conductivity of the membrane especially at elevated temperatures (>80°C) [10,11]. Moreover, the single cell operating at relatively low temperatures (<80°C) faces with some other challenges, including sluggish kinetics of oxygen reduction and methanol oxidation reactions and less catalyst contamination (CO poisoning) tolerance [12]. When the operating temperature reaches elevated levels (>80°C), the reaction kinetics increase and the risk of CO poisoning decreases [13]. Considering these facts, it is expected that operating at elevated temperatures (>80°C) would increase DMFC performance significantly, if suitable MEA materials could be used. Therefore, in order to take advantage of high temperature operation, the membrane needs to fulfill some desired properties, including high proton conductivity, thermal and chemical stability, and low fuel permeability even at elevated operating temperatures [14].

There has been an ongoing research in the area of development of alternative membranes to circumvent the problem of membrane dehydration. Some alternative membranes, which possess an improved water retention ability and thermal stability at elevated temperatures (>80°C), have been developed and investigated [15,16]. Several approaches have been extensively used in the manufacturing process of these alternative membranes, including incorporation of some metal-oxide particles (e.g., TiO₂, SiO₂, TiSiO₄, and ZrP) into the Nafion[®] matrix to improve the proton conductivity, water retention properties, and thermal and chemical stability of the bare Nafion[®] membrane. For instance, Devrim et al. [10] manufactured Nafion/TiO₂, Nafion/SiO₂, and Nafion/nanosize titanium silicon oxide (TiSiO₄) composite membranes using ultrasonic spraying technique and conducted some experimental studies to determine the performances of these composite membranes in the proton exchange membrane fuel cells (PEMFCs). The results of their study showed that Nafion/TiSiO₄ composite membrane yields better performance as compared to Nafion[®], Nafion/TiO₂, and Nafion/SiO₂ membranes. They also reported that the composite membranes are very promising for PEMFCs due to their superior water retention and uptake abilities at elevated operating temperatures. Jalani et al. [17] synthesized Nafion/ZrO₂, Nafion/SiO₂, and Nafion/TiO₂ nanocomposite membranes by sol-gel method for high temperature PEMFCs and characterized them using Thermogravimetric Analysis (TGA) and Dynamic Mechanical Analysis (DMA). Their goal for synthesizing these composite membranes was to develop membranes, which have high proton conductivity and appropriate water retention and thermo-mechanical properties. The results of their TGA and DMA showed that the nanocomposite membranes have superiority as regards degradation and glass transition temperature over bare Nafion[®]. Other types of Nafion[®] based composite membranes which have been synthesized for fuel cell applications include but not limited to Nafion/ PTFE [18-20], Nafion/PVA [21], and diisopropyl phosphite/Nafion [22].

According to our literature survey, Nafion[®] based composite membranes, especially Nafion/ZrP composite membranes, are considered to be of “highly promising”, especially for overcoming the problem of dehydration and increasing the proton conductivity of the membrane at relatively high operating temperatures. For example, Yang et al. [13] prepared Nafion/ZrP composite membrane and investigated the performance of the PEMFC based on this membrane. They also made performance comparison between the PEMFC having a Nafion/ZrP composite membrane and PEMFC having an unmodified Nafion[®] membrane under various operating conditions. They reported that the Ohmic resistance of the Nafion/ZrP composite membrane at elevated temperatures (130°C-140°C) was dramatically less than that of unmodified Nafion[®] membrane. The PEMFC with a Nafion/ZrP composite membrane showed much higher current density in comparison to PEMFC having unmodified Nafion[®] membrane at temperatures above 100°C. It was also reported that the performance values of both of the PEMFCs at 80°C were almost same. Costamagna et al. [23] investigated the composite Nafion/ZrP

composite membranes for high temperature PEMFCs. The results of their study demonstrated that the PEMFC having Nafion/ZrP composite membrane gave 1500 mA/cm² at the operating conditions of 130°C and 3 bar. It was also stated that the Nafion/ZrP composite membrane exhibited highly stable behavior at 130°C.

Another important component of MEA is the catalyst, which has a significant effect on the performance of a fuel cell. Conventionally, carbon supported or unsupported Pt-Ru and Pt have been used as the catalyst for the anode and cathode sides of DMFC, respectively. However, Pt cathode catalyst causes some problems (e.g., performance loss due to CO poisoning and sluggish reaction kinetics at the cathode and an increase in the material cost) for DMFCs. Recently, researchers have started to pay more attention to the investigation of some Pt-based alternative cathode catalysts, such as Pt-Co, Pt-Pd, Pt-Fe, and Pt-Au to alleviate the negative effects associated with these problems. These Pt-based alternative cathode catalysts have been proven to be effective and are considered to be state-of-the-art catalysts due to their significant characteristics, including the ability to decrease the active areas for methanol adsorption at the cathode side, to reduce undesired methanol oxidation at the cathode, and to achieve relatively higher catalytic activity for oxygen reduction [24-26]. For instance, Xu et al. [27] and Selvarani et al. [28] investigated the effect of Pt-Au alloy cathode catalyst on the performance of DMFCs and they reported that the power density of the DMFC having Pt-Au/C cathode catalyst is almost twice as much as the MEA having conventional Pt/C cathode catalyst. Shukla and Raman [24] investigated the effect of different methanol resistant oxygen reduction catalysts, including Pt-Fe/C and Pt-Co/C on the performance of DMFCs. They reported that these catalysts could be a good solution for mitigating the performance losses in the DMFCs that take place through methanol crossover from the anode to cathode. Owing to these composite cathode catalysts, significant progress in improving the performance of DMFCs has been achieved; however, there are still some challenges as regards improving the rate of oxygen reduction reaction (ORR) at the cathode. This challenge could be ironed out incorporating additives (e.g., zirconium hydrogen phosphate (ZrP)) into the cathode catalyst. Due to its layered structure, high proton conductivity arising from high proton mobility notably on the surface of ZrP [29], comparatively high hygroscopicity at elevated temperature operation, and cation exchange features [30], ZrP could be used as a temperature-proof solid electrolyte to maintain proper proton conductivity at elevated operating temperatures [31].

The literature survey discussed above demonstrates that Nafion/ZrP composite membranes may have a great potential for being used as state-of-the-art material for DMFCs, notably at elevated operating temperatures (>80°C). Although there has been some studies conducted for PEMFCs based on these materials in the literature, there is no significant study comparing the performance of DMFCs having Nafion/ZrP composite membranes (made of different ZrP weight ratios) with DMFCs having Nafion[®] membranes. In addition, to the best of our knowledge, there is also no work related to the comparison of DMFCs having both Pt/C-ZrP cathode catalyst and Nafion/ZrP composite membrane with DMFC made of conventional materials. Hence, in this study, the effect of Nafion/ZrP composite membranes on the performance of DMFCs was compared with that of DMFC having commercial Nafion[®] 115 membrane. The performance comparison studies of these DMFCs were conducted at different temperatures (40°C, 60°C, 80°C, and 100°C) and methanol concentrations (0.75 M, 1.00 M, and 1.50 M). In addition, the performance of the DMFC based on Pt/C-ZrP cathode catalyst and Nafion/ZrP membrane was compared with that of the DMFC based on the same membrane but the conventional Pt/C cathode catalyst at the same temperatures and methanol concentrations. In addition, 4 h short-term stability tests were conducted for all the manufactured MEAs to assess their stability characteristics.

2. Experimental

2.1. Materials

Two different commercially available cathode catalyst powders were purchased: 1) Platinum, nominally 60% on high surface area advanced carbon support, HiSPEC[®] 9100 from Alfa Aesar[®] (Karlsruhe, Germany) and 2) HP 60 wt.% Pt on Vulcan XC-72. The commercially available anode catalyst powder (HP 60 wt.% Pt-Ru on Vulcan XC-72) was used as anode catalyst. The commercially available Teflon treated carbon cloth (ELAT LT1400W) used as anode backing layer was obtained from Nuvant Systems Inc. (Crown Point, IN, USA) and used as received. Nafion[®] 115 membrane was purchased from DuPont Corp. (Delaware, USA). 15 wt.% Nafion solution

(equivalent weight = 1100 g mol⁻¹ SO₃H) was obtained from Ion Power Inc. (Delaware, USA). Hydrogen peroxide (Emsure[®], chemical purity 30 wt.%) and sulphuric acid (Emsure[®], chemical purity 95-97 wt.%) were obtained from Merck (Darmstadt, Germany) and used without further purification. N-N Dimethylacetamide (DMAc), was purchased from Merck (Germany). Zirconium hydrogen phosphate (ZrP) was obtained from ChemCruz[®] Biochemicals (USA). All solvents used were high grade materials without further need for purification. All chemicals, including isopropyl alcohol (Aldrich) and methanol (Aldrich), were of reagent grade and used without further purification.

2.2. Membrane preparation and characterization

Nafion/ZrP nanocomposite membranes were prepared using the recasting method. A total of 15 wt.% Nafion solution was evaporated at 70°C until a dry residue was obtained. Nafion resin was redissolved in DMAc to form a solution containing 5 wt.% Nafion. Appropriate amount of ZrP powder was added to achieve better dispersion of ZrP particles and then the mixture was sonicated for an hour. Resulting mixture was cast onto petri dishes and the solvent evaporated at 80°C. The membrane was removed from the petri dish by wetting with de-ionized water.

Thermal stability of the membranes was determined by TGA method, with Perkin Elmer Pyris 1 TGA Equipment. Temperature range was 25°C-800°C with heating rate of 10°C/min under nitrogen atmosphere.

The crystal structures of the membranes were determined by X-Ray Diffraction (XRD) analysis, using Bruker D8 Advance equipment, over the range 5° ≤ 2θ ≤ 80°.

The membrane and cathode and anode catalyst layer morphologies were observed by Scanning Electron Microscope (SEM), QUANTA 400F Field Emission SEM system equipped with an energy dispersive X-ray (EDX) spectrometer. Before measurements, the samples were coated with a layer of gold to enhance electrical conduction. Membrane samples were prepared by freezing the membranes in liquid nitrogen and then fracturing them for cross-section SEM images.

Water uptake is considered as one of the most important characteristic properties for proton exchange membranes, which confirms the successful incorporation of hydrophilic groups inside the membrane. For water uptake measurements, membranes were dried in a vacuum oven at 100 °C for 6 h and weighed. Then, the samples were immersed in distilled water for 24 h. Excess water was gently wiped off with a tissue and membrane samples were weighed immediately. The water uptake was calculated using Eq.(1) [32].

$$\text{Water Uptake} = \left[\frac{W_{\text{wet}} - W_{\text{dry}}}{W_{\text{dry}}} \right] \times 100 (\%) \quad (1)$$

Where W_{wet} and W_{dry} are the weights of the water-swollen and dry membrane sample, respectively.

Proton conductivities of the membranes were determined by electrochemical impedance spectroscopy (EIS), four probe method, using ZIVESP2 Electrochemical Workstation. Four probe method consists of four equally spaced (1 cm for each space) Pt probes. The membranes were cut to fit in the measurement cell so that it interacts with all four probes. AC impedance was measured between 30 MHz and 65 mHz for all the membranes. The measurements were conducted under five different temperatures, 25°C, 50°C, 60°C, 70°C, and 80°C. All the measurements were performed in longitudinal direction; in air/water vapour atmosphere with 100% relative humidity. Equation used for calculation of conductivity is given in Eq. (2).

$$\sigma = \frac{L}{R \times w \times t} \quad (2)$$

In this equation σ is the proton conductivity of the membrane (S cm⁻¹), R is the resistance value for the membrane (Ω), w is membrane width (cm), t is the membrane thickness (cm), and L is the gap between two probes of the impedance cell (cm). In order to confirm the reproducibility of the results, at each temperature, corresponding proton conductivity data were collected for about an hour.

Using the conductivity data, activation energies were calculated by Arrhenius equation. Ion transport activation energies were calculated from Arrhenius equation shown in Eq. (3) [33]:

$$\sigma = \sigma_0 \exp\left(\frac{-E_a}{RT}\right) \quad (3)$$

Where σ (S cm⁻¹), σ_0 (S cm⁻¹), E_a (Jmol⁻¹), R (J mol⁻¹ K⁻¹), and T (K) denote the ionic conductivity, frequency factor, activation energy for conduction, universal gas constant, and temperature, respectively.

2.3. MEA manufacturing

The first step in the MEA manufacturing process is the catalyst ink preparation process. In this process, two different catalyst inks were prepared for the anode and cathode sides to be used in air spraying technique. For this purpose, appropriate amounts of catalyst powder, deionized water, Nafion® solution, and isopropyl alcohol were consecutively mixed by a magnetic stirrer and ultrasonic bath for 30 min and 3 h, respectively. However, to prepare the Pt/C-ZrP cathode catalyst ink, 10 wt.% of ZrP with respect to the amount of cathode catalyst (Pt/C) was added directly to the prepared mixture just before mixing process. Then, the backing layers (carbon cloth for anode and carbon paper for cathode) were placed on a heated-vacuum table (at 50°C) and the prepared inks were sprayed through an air spray gun. The spraying continued until the catalyst loadings of the anode and cathode sides reached to a desired value (4 mg_{PtRu}/cm² for the anode and 4 mg_{Pt}/cm² for the cathode). The active areas of the backing layers were taken as 25 cm². After the coating, the coated backing layers were dried at the room temperature. As the last step in the MEA manufacturing process, the hot-press process was applied. In this process, the membrane dictated by the test of interest (Nafion® 115 or Nafion/ZrP composite membrane) was located between the coated anode and cathode backing layers and pressed at 120°C and 6.89 MPa for 4 min [34,35]. The composition of all the MEAs prepared for testing is summarized in Table 1.

Table 1. Specifications of the MEAs.

MEA	Membrane Type	wt.% ZrP in Membrane	Catalyst Type	Anode Loading (mg _{PtRu} /cm ²)	Cathode Loading (mg _{Pt} /cm ²)	wt.% ZrP in the cathode catalyst
MEA-1	Nafion® 115	0	HP	4	4	0
MEA-2	NZ-2.5	2.5	HP	4	4	0
MEA-3	NZ-5	5	HP	4	4	0
MEA-4	NZ-2.5	2.5	HiSPEC® 9100	4	4	0
MEA-5	NZ-2.5	2.5	HiSPEC® 9100	4	4	10

2.4. Performance testing

The performances of the MEAs manufactured using the procedure discussed in Section 2.3 were tested through in-house experimental studies. Before the experiments, the channels of the flow-field plates were cleaned using a soft brush to remove the undesired inorganic particles. Then, two gaskets with the thicknesses of 0.1 mm were placed to the anode and cathode sides to prevent the cell from leakage problem. The MEA located between the gaskets was compressed applying a compression torque, which was increased gradually until a desired value of relative MEA compression ratio (Eq. (4)) was achieved. For this study, this ratio was considered as 20 ± 5% [36]. In this equation, uncompressed MEA thickness was calculated taking the average values of 9 different points within the active area of the MEA.

$$\text{Relative MEA Compression (\%)} = \frac{(\text{Uncompressed MEA thickness}) - (\text{Compressed MEA thickness})}{(\text{Uncompressed MEA thickness})} \quad (4)$$

After the MEA was placed to the single cell, a series of in-house experiments were carried out using a computer-aided DMFC test station. The schematic of the test station is shown in Fig.1. The operating principle of the test station can be summarized as follows. Methanol flows through the magnetic gear pump before it enters the cell, whereas oxygen first flows through the micro-flow controller and then enters the humidifier. Humidified oxygen

enters the cell in order to keep the cathode side of the membrane hydrated. In addition, to keep the temperature inside the cell at a desired value and uniform, several heaters are placed before the anode and cathode inlets and also on the top and bottom of the cell. At the cathode outlet, the products are passed through a separator to separate the liquid and gas streams before they enter the back pressure regulator.

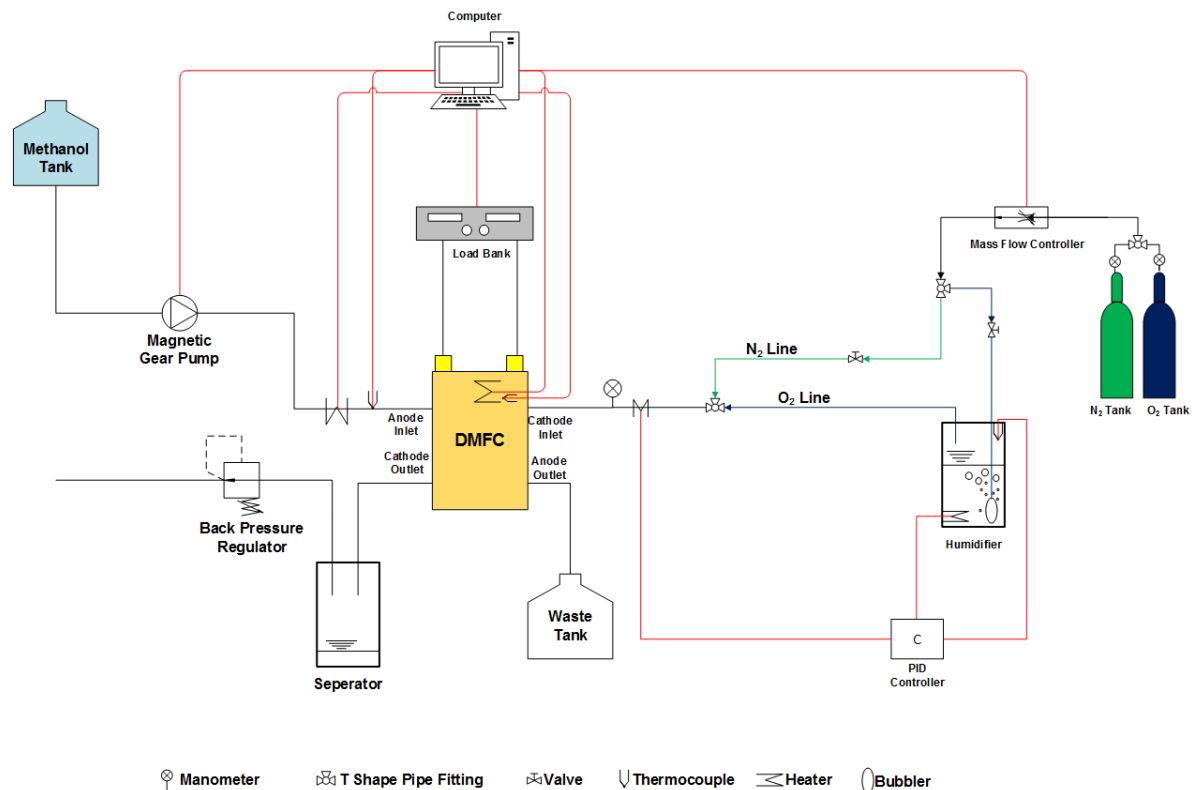


Fig.1. The schematic of the computer aided DMFC test station.

At the beginning of the experiments, the pretreatment procedure was carried out to make the membrane well-hydrated and the MEA ready for performance testing procedure. Towards this direction, deionized water with the flow rate of 5 ml/min and humidified oxygen with the flow rate of 1000 ml/min were passed through the anode and cathode flow channels, respectively, for 3 h. The pressure at the cathode inlet of the cell was kept at 1.35 bar using a pressure regulator. Once the pretreatment procedure was completed, the flow rates of the humidified oxygen and methanol solution were set to 200 ml/min and 1.94 ml/min, respectively. After the open circuit voltage (OCV) was achieved, several voltage steps (between OCV and 0.2 V) interrupted by OCV steps were applied. Several polarization curves were generated recording the current density at each voltage step. This process continued until the difference between two consecutive curves became negligible. The values at the last iteration were used for plotting the polarization curve of that specific experiment. Once all the relevant data were obtained, the flow rates of the humidified oxygen and methanol solution were set to zero, and nitrogen gas was sent through the flow channels to dry the fully soaked membrane and the flow channels.

3. Results and Discussion

3.1. Characterization of the Nafion-115 and Nafion/ZrP Nanocomposite membranes

3.1.1. Thermal Stability (TGA)

The results of the thermal stability measurements for the Nafion and Nafion/ZrP composite membranes are presented in Fig.2. It was observed that all the membranes retain more than 90% of its weight up to a temperature of about 300°C. The results of the thermal degradation of Nafion membranes agree well with the

results from literature [37]. The first weight loss, between 50°C and 200°C, corresponds to moisture removal from the membranes. Second weight loss region between 200°C-400°C indicates the degradation of $-\text{SO}_3\text{H}$ groups (Fig.2). The last weight loss region was observed between 400°C and 550°C and this was related to the decomposition of Nafion (Fig.2, inset) [38]. Thermal decomposition behavior of Nafion/ZrP composite membranes was similar to that of pristine Nafion membrane. However, the decomposition temperature of the polymer main chain was shifted to a slightly higher temperature with the addition of 5 wt.% ZrP. Major polymer main chain decomposition temperature for pristine Nafion was spotted at about 425°C, while NZ-5 membrane showed decomposition at approximately 430 °C (Fig.2, inset). This shows that zirconium phosphate with a layered structure may lead to an increase in thermal degradation temperature [39].

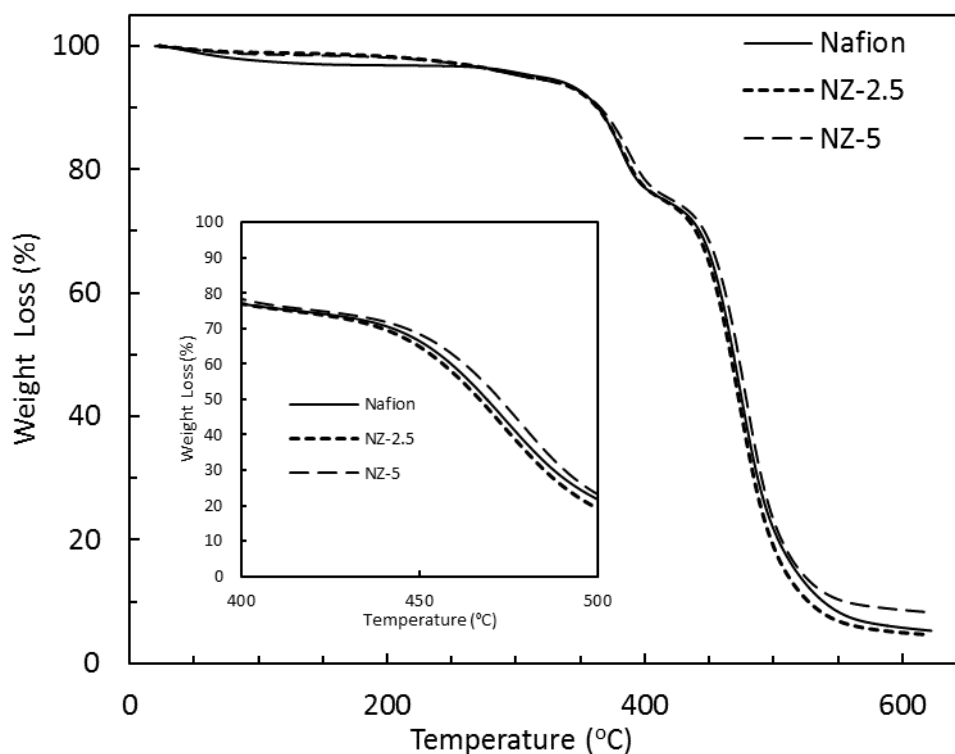


Fig.2. TGA curves of the Nafion and Nafion/ZrP composite membranes.

3.1.2. XRD Study

XRD patterns of Nafion, Nafion/ZrP composite membranes, and ZrP particles are illustrated in Fig.3. The bare Nafion membrane shows two main peaks at $17.5^\circ (2\theta)$ and $38.3^\circ (2\theta)$ (Fig.3), which are consistent with those reported in literature [39]. The broad peak at $17.5^\circ (2\theta)$ was related to the crystalline scattering of the polyfluorocarbon chains in membranes, which overlapped the X-ray scattering from the amorphous region of the membrane at lower Bragg angles.

The XRD pattern of ZrP particles shows very weak diffraction peaks at $21.11^\circ (2\theta)$ and $26.73^\circ (2\theta)$ (Fig.3, inset), thus ZrP particles can be defined as amorphous. NZ-2.5 showed no discrete, sharp reflexes which indicates that there were no structural changes in polymer matrix. NZ-5 membrane also showed no sharp peaks indicating structural changes in XRD results. These were the expected results since the particles used were also amorphous.

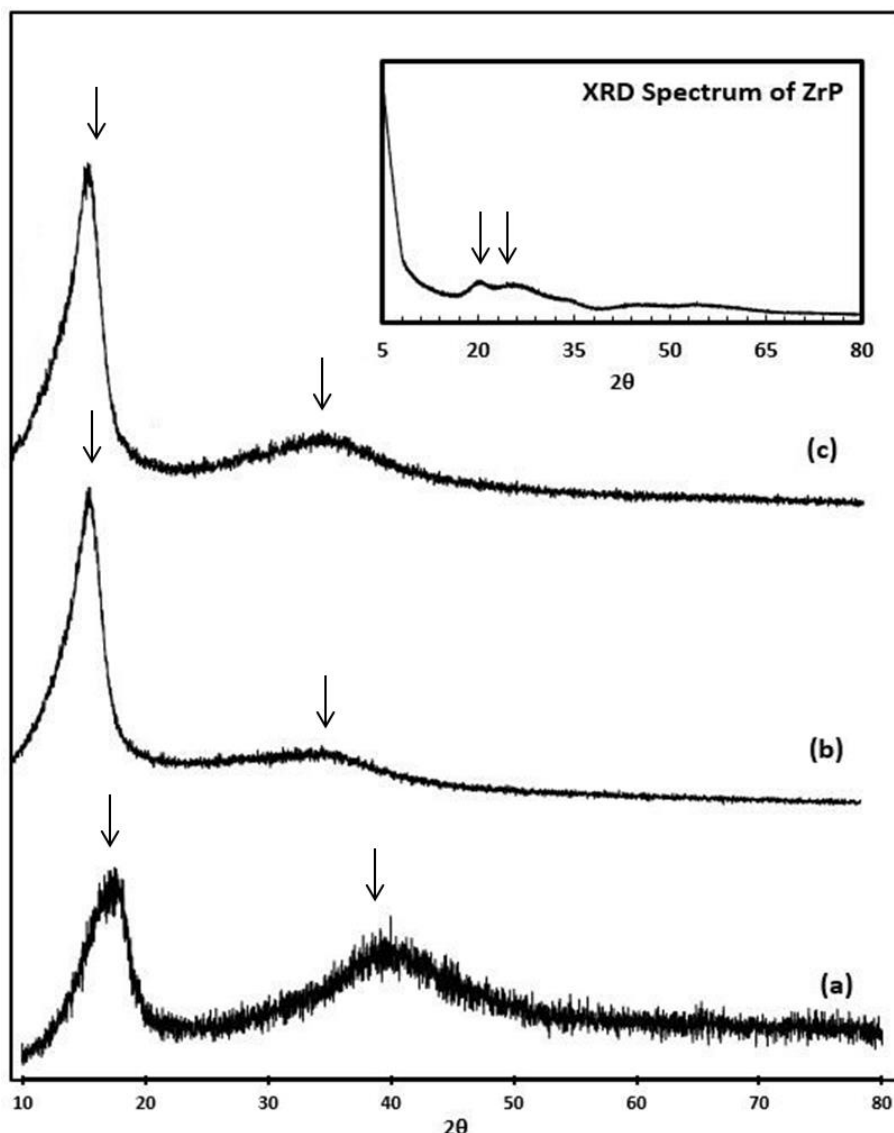


Fig.3. XRD spectrums of (a) Nafion membrane, (b) NZ-2.5, and (c) NZ-5 and ZrP nano particles.

3.1.3. SEM analysis

Scanning electron microscopy (SEM) was used to investigate the microstructure of the bare Nafion membrane as well as those of the composite membranes with different contents of ZrP. The morphological properties of the composite based membranes depend on the degree of compatibility and dispersibility between the polymer and filler. Fig.4 shows the SEM images of the bare Nafion and Nafion/ZrP nanocomposite membranes. Fig.4(a) shows the surface of the pristine Nafion membrane. The surface of the Nafion membrane presents a smooth surface without any cracks or pinholes. As seen from Figs.4(b) and (c), slight agglomerations were observed in the NZ-5 membrane matrix. This result can be attributed to the incompatibility of ZrP with Nafion at high ZrP loadings. Figs. 4(d) and (e) display the cross-section image of the Nafion/ZrP membrane with 2.5 wt.% ZrP loading. As seen from Figs.4(d) and (e), ZrP particles are uniformly distributed within the composite membrane as a result of the interaction between the Nafion polymer and ZrP. It is worthwhile to note that no big agglomerates are visible, which means ZrP particles can be dispersed homogeneously in the polymeric matrix for NZ-2.5 composite membrane. This indicates the effectiveness of compatibility for ZrP embedded into the polymer matrix [40]. The thicknesses of the composite membranes were around $64 \pm 5 \mu\text{m}$ (Figs. 4(c) and (e), insets).

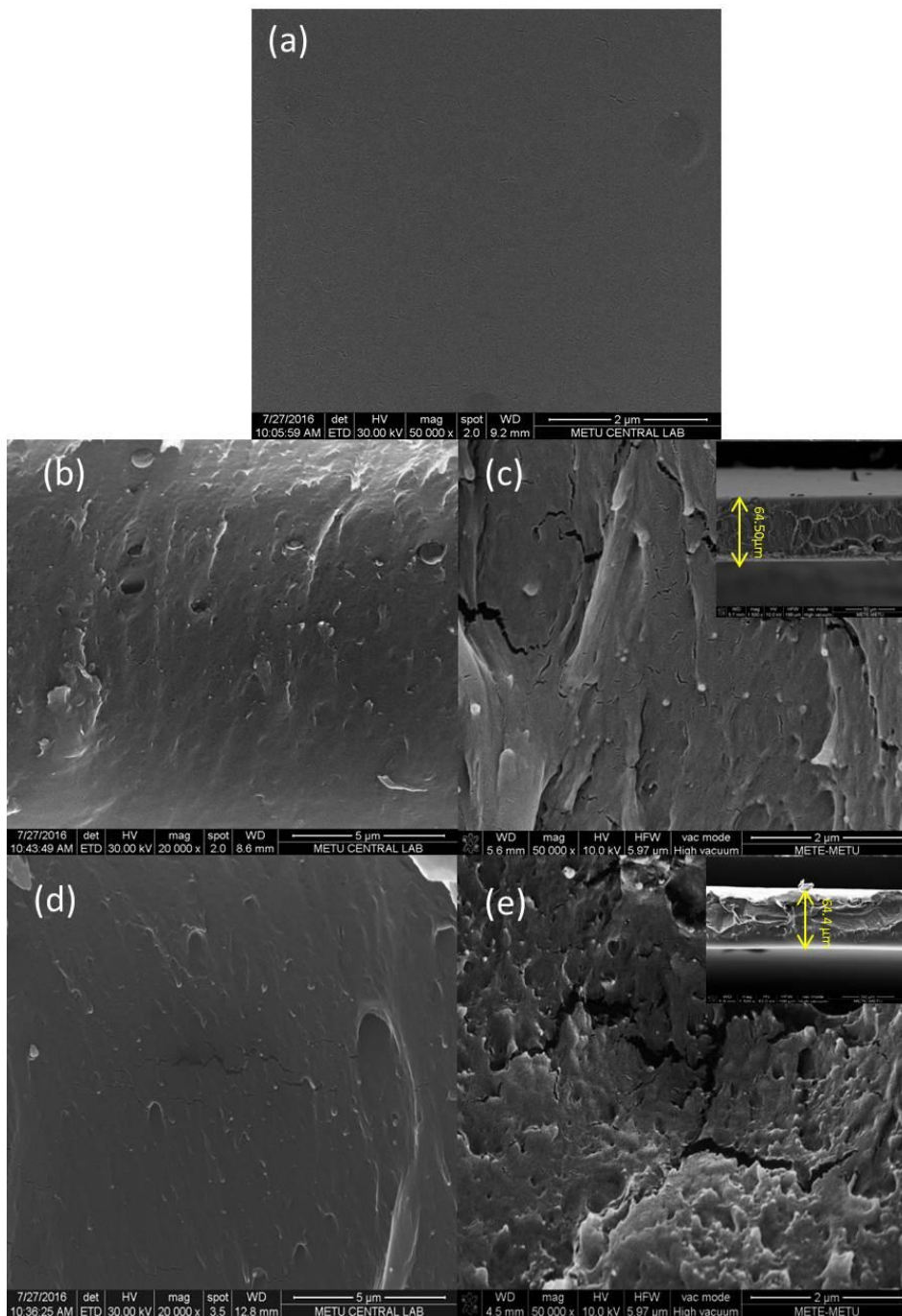


Fig.4. SEM images of (a) Nafion membrane (x50000), (b) NZ-5 (x20000), (c) NZ-5 (x50000), (d) NZ-2.5 (x20000), and (e) NZ-2.5 (x50000) membranes.

EDX spectrum of Nafion and Nafion composite membranes are shown in Fig.5. EDX spectrum of pure Nafion membrane is shown in Fig.5(a). The spectrum shows the presence of carbon (C), oxygen (O), sulphur (S), and Fluorine (F). Figs.5(b) and (c) show the EDX spectrums of the composite membranes. EDX spectrums of Nafion/ZrP nanocomposite membranes confirm the presence of ZrP particles reside in the composite membranes. The peaks are the reflection of the presence of Zr, C, O, S, and F components in the composite membranes, which is the evidence of that ZrP particles added to the polymer solution were fixed in the polymer network.

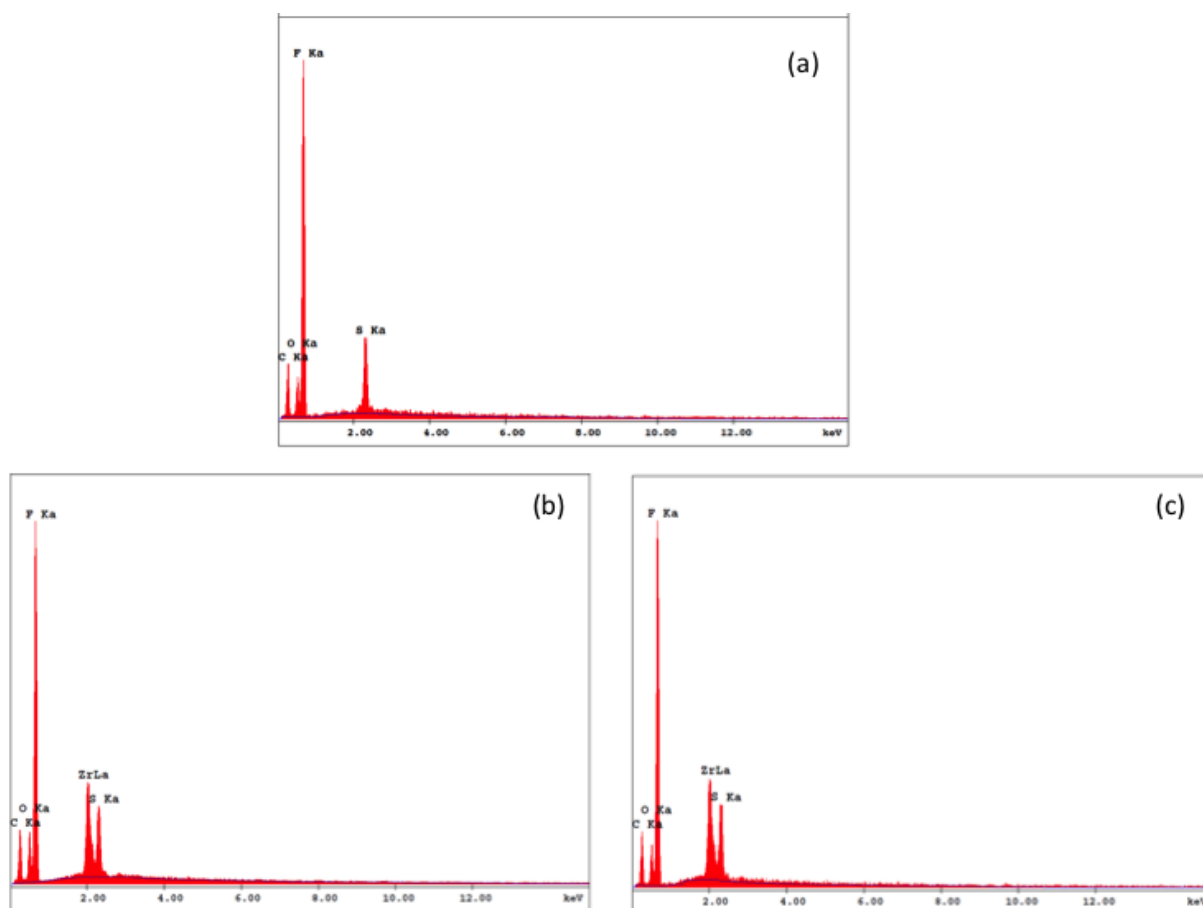


Fig.5. EDX spectra of (a) Nafion, (b) NZ-2.5, and (c) NZ-5 membranes.

3.1.4. Water Uptake

Water uptake plays a significant role in proton exchange membrane characterization. The hydration of the membrane is closely related to the proton conductivity. To investigate the effect of ZrP nano particles on the water retention capability of the Nafion/ZrP composite membranes, water uptake tests were conducted. Water uptake values for Nafion[®] 115, NZ-2.5, and NZ-5 membranes are represented in Table 2. Nafion[®] 115 showed the lowest water uptake value amongst the membranes. As the ZrP loading increased from 2.5 wt.% to 5 wt.%, water uptake percent increased from 11 to 13.3. These results indicate that addition of ZrP particles contributes to the water retention capability of membranes. ZrP increases the water content of the membranes due to its disruption of the cohesive forces of Nafion. Additionally, ZrP particles interact with Nafion polymer probably through hydrogen bonding between $-\text{SO}_3\text{H}$ groups, which are combined with the increase of the water uptake and the water mobility. These findings are compatible with literature [41,42].

3.1.5. Proton Conductivity

Electrochemical Impedance Spectroscopy (EIS) was conducted to determine the proton conductivities of the membranes. The proton conductivities of the Nafion[®] 115 and Nafion/ZrP composite membranes at five different temperatures were measured. Since temperature plays a vital role in proton conduction kinetics and the mobility of polymer chains, all the membranes exhibited an increase in the proton conductivity as the temperature increased. High temperature promotes the dissociation of hydrogen which results in higher conductivity values. The results showed that introducing ZrP to polymer matrix enhanced proton conductivity values of Nafion membrane. At temperatures 25°C, 50°C, 60°C, and 70°C, NZ-2.5 membrane exhibited the highest proton conductivities amongst the samples. At 80°C, however, NZ-5 had higher proton conductivity with the value of 0.223 S/cm (Table 2). The improved proton conductivity of nano composite membranes can be explained by the layered structure of ZrP. Each zirconium atom is coordinated with six oxygen atoms belonging to six different

OH-PO₃ groups. This is a group of inorganic proton conductors that show high proton conductivity [43]. The proton conductivity increase can also be explained by hydrophilicity of ZrP particles. ZrP particles supply additional proton conducting moieties in the membrane. Water uptake plays an important role in proton conductivity. As the water uptake values become higher, the number of interconnecting channels between ionic groups also increases for the protons to use to cross the membrane. All the membranes exhibited an increase in conductivity with temperature. At temperatures lower than 80 °C, NZ-5 membrane had lower proton conductivity values compared to NZ-2.5 membrane. This can be attributed to slight agglomerations of ZrP particles in NZ-5 membrane which were observed in SEM pictures (Fig.4). At 80 °C, NZ-5 membrane shows slightly higher proton conductivity value than NZ-2.5. This may be related to the fact that at higher temperatures water dilution is an obstacle, and higher hydrophilic ZrP particle incorporation reduces water dilution and stabilizes dimensional swelling at higher temperatures [44,45].

Table 2. Conductivity, activation energy and water uptake data for Nafion-115 and Nafion/ZrP composite membranes.

Membrane type	Activation Energy (kJ/mol)	Water Uptake (%)	Proton Conductivity (S/cm)				
			25°C	50°C	60°C	70°C	80°C
			Nafion® 115	10.7	10.1	0.081	0.107
NZ-2.5	15.4	11.0	0.101	0.175	0.206	0.213	0.218
NZ-5	19.5	13.3	0.078	0.140	0.172	0.198	0.223

Activation energies and conductivity values obtained are shown in Table 2. In the Nafion-based membranes, the proton conduction is dominated by the Grothuss mechanism. In this mechanism, the proton which forms as H₃O⁺ ion jumps to the neighboring lone pair of electrons of a water molecule. For such a mechanism, the activation energy for proton conduction should be around 14-40 kJ mol⁻¹. The results are compatible with these values; therefore, it can be concluded that the proton conduction mechanism is dominated by Grothuss mechanism. E_a values for composites with ZrP particles are higher than that for pristine Nafion membrane. This may be explained by the addition of inorganic fillers to the polymer matrix [46]. Nano fillers act as a carrier-bridge; thereby, this process requires more energy. Although the activation energies for nanocomposite membranes were found to be higher than that for Nafion® 115 membrane, proton conductivity of the nanocomposite membranes is higher than that of Nafion® 115. This is due to the increased hydrogen bonding by introduction of ZrP particles to the polymer matrix. Hydrogen bondings act as a proton conduction channel and improve proton conduction of the membranes. Additionally, since incorporation of ZrP increases water uptake, proton conductivity becomes higher in nanocomposite membranes [47].

3.2. SEM Analysis of Cathode and Anode Catalyst Layers

The cell performance of MEA is strongly dependent on the pore structure of the electrodes. Fig.6 shows SEM surface images and EDX spectras of the anode and cathode electrode structures. As shown in SEM images, no agglomerates are visible for all electrodes. This means that ZrP and Pt/C particles are homogeneously dispersed in the electrodes. Electrodes also showed no cracks or mud-like morphologies. As seen from EDX spectra in Fig.6(b), C, O, S, F, Pt, and Zr peaks were detected for cathode catalyst layer. This can be attributed to the presence of ZrP in the cathode electrodes. Figs.6(d) and (f) show the C, O, S, F, and Pt peaks for the cathode and anode electrode without ZrP filler, respectively.

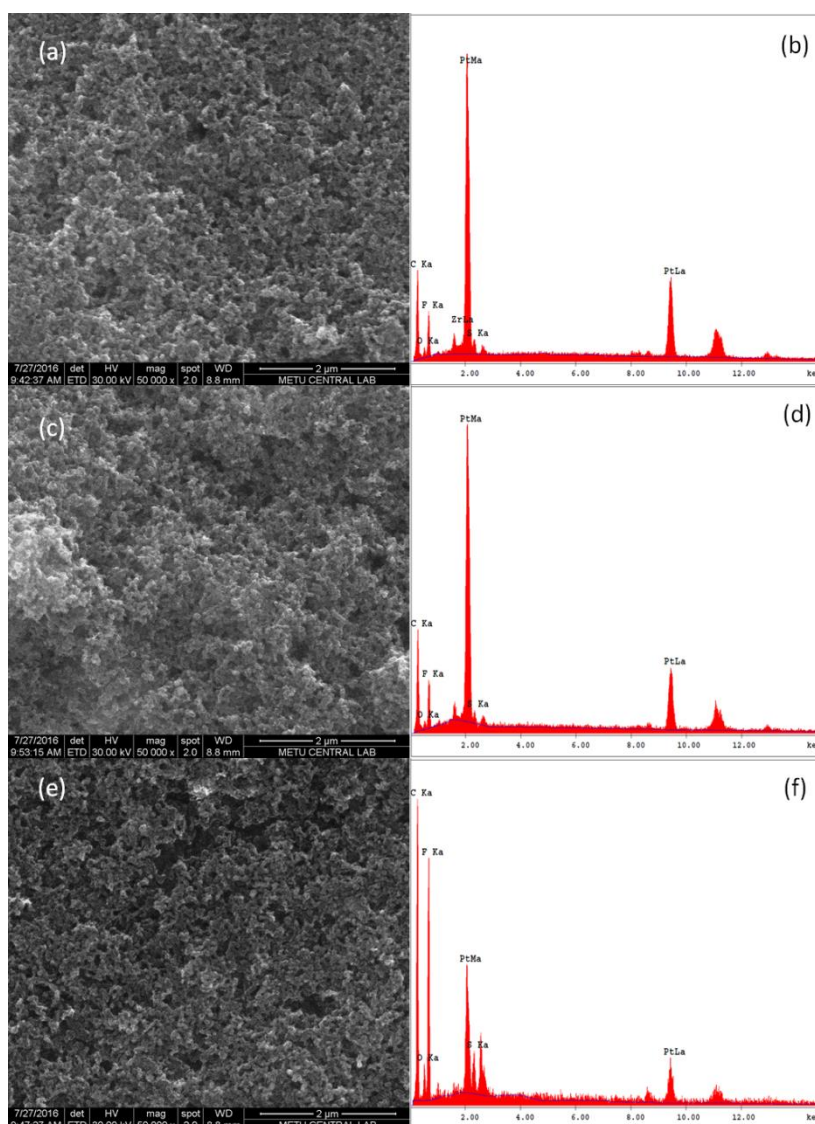


Fig.6. SEM surface images of (a) Cathode catalyst layer with ZrP, (c) Cathode catalyst layer without ZrP, (e) Anode catalyst layer, and EDX spectrums of (b) Cathode catalyst layer with ZrP, (d) Cathode catalyst layer without ZrP, (f) Anode catalyst layer.

3.3. Performance testing of the MEAs

Three different MEAs with 25 cm² active areas were fabricated using air-spraying technique as mentioned in Section 2.3. The differences in these MEAs mainly originate from using different membranes: commercial Nafion® 115 membrane, NZ-2.5, and NZ-5. In this section, the effects of operating temperature, supplied methanol concentration, and type of cathode catalyst on the performance of the DMFCs are discussed. In addition, the stability characteristics of these DMFCs are both presented and interpreted.

3.3.1. Effect of operating temperature

Operating temperature is one of the main parameters that affects the performance of these MEAs [33]. Fundamentally, the increase in the operating temperature of DMFCs results in several adverse effects: an increase in the reaction kinetics at both the anode and cathode, an improvement in the ionic conductivity of Nafion membranes, a deterioration in the water retention capability of the membrane, and a triggering of the undesired methanol crossover from the anode to cathode [48,49]. Therefore, in spite of the fact that the increase in the operating temperature causes some opposite effects as mentioned above, the overall performance of DMFCs generally improves with increasing operating temperature until a certain temperature value. After a

certain operating temperature value, the previously mentioned negative effects (e.g., methanol crossover and dehydration of membrane) become more dominant, leading to a deterioration in DMFC performance significantly. As the usage of Nafion/ZrP composite membranes and introduction of ZrP to the cathode catalyst could potentially change the compound effect, the experimental studies were conducted at different operating temperatures (40°C, 60°C, 80°C, and 100°C) and the methanol concentration of 1.00 M. The results of the experiments conducted for investigating the effect of the operating temperature on the performance of MEA-1 are shown in Fig.7(a). As seen from Fig.7(a), the maximum power density was found as 537.48 W/m² at 80°C and 1.00 M methanol concentration. In addition, the peak power densities at 40°C, 60°C, and 100°C (for 1.00 M methanol concentration) were found as 239.52 W/m², 362.64 W/m², and 441.36 W/m², respectively.

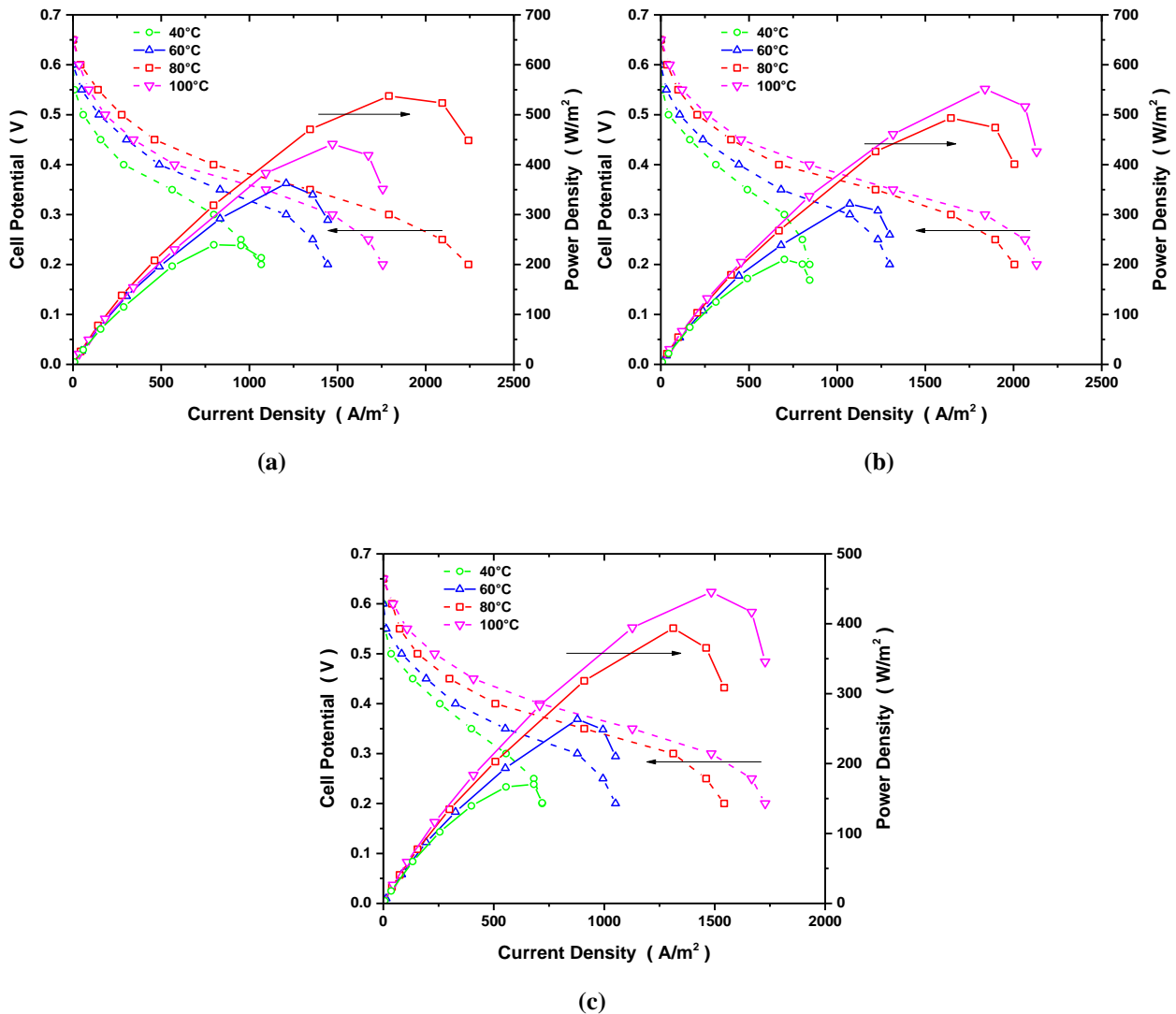


Fig.7. Power density and polarization curves at 40°C, 60°C, 80°C, 100°C and 1.00 M methanol concentration for (a) MEA-1, (b) MEA-2, and (c) MEA-3.

As can be seen in Fig.7(a), the best performance of MEA-1 was achieved at 80°C as expected. The experiments conducted for MEA-1 were repeated for MEA-2 and MEA-3 to compare the performances of these two MEAs with that of MEA-1. Figs.7(b) and (c) present the power density and polarization curves of MEA-2 and MEA-3 at these temperatures, respectively. As can be seen from Fig.7(b), the maximum power density of MEA-2 was achieved as 551.52 W/m² at 100°C and 1.00 M. In addition, the peak power densities at 40°C, 60°C, and 80°C and 1.00 M were found as 210.24 W/m², 321.36 W/m², and 493.44 W/m², respectively. As seen from Fig.7(c), the best performance of MEA-3 was achieved as 445.44 W/m² at 100°C, whereas the peak power densities at

40°C, 60°C, and 80°C (for 1.00 M methanol concentration) were found as 166.68 W/m², 263.52 W/m², and 393.72 W/m², respectively.

As seen from Figs.7(a)-(c), when the operating temperature increases from 40°C to 80°C, the performances improve as expected. More specifically, for this increase of temperature, the peak power densities increase from 239.52 W/m² to 537.48 W/m², 210.24 W/m² to 493.44 W/m², 166.68 W/m² to 393.72 W/m² for MEA-1, MEA-2, and MEA-3, respectively. The reason of the performance improvement as the operating temperature increases from 40°C to 80°C could be related to the increase in the electrochemical reaction kinetics at both the anode and cathode as well as to the significant enhancement in the proton conductivity of both the bare Nafion[®] membrane and Nafion/ZrP composite membranes. However, as the operating temperature increases from 80°C to 100°C, the maximum power density value of MEA-1 decreases from 537.48 W/m² to 441.36 W/m². The reason of the performance deterioration as the operating temperature becomes higher may be related to the dehydration problem of commercial Nafion[®] 115 membrane, which leads to a significant deterioration in the proton conductivity of the membrane. The increase in the operating temperature also triggers the undesired methanol permeation from the anode to cathode by increasing the diffusion of methanol through the membrane which in turn decreases the performance of the cell [10]. In addition, as the operating temperature reaches to 100°C, the chemical stability of the bare Nafion[®] membrane deteriorates. In contrast, the peak power density values of MEA-2 and MEA-3 increase from 493.44 W/m² to 551.52 W/m², 393.72 W/m² to 445.44 W/m², respectively, for the same temperature increment. This performance improvement is consistent with those reported in literature [23,31] and can be explained by the fact that the chemical stability and water retention ability of Nafion/ZrP composite membranes enhance as the temperature reaches to 100°C [42]. In addition, the methanol impermeability characteristic of Nafion/ZrP composite membranes is much more advanced in comparison to Nafion[®] 115 membrane [50], thus reduces the amount of crossed-over methanol at the cathode and eventually improves the performance as the temperature increases. Given these facts, Nafion/ZrP composite membranes seem more promising as compared to Nafion[®] 115 membrane, specifically regarding chemical and physical stability, methanol impermeability, and water retention ability during the high-temperature operation. There is also a more subtle point that must be considered is that high temperature operation (e.g., 100°C) provides a significant advantage with regard to improvement in the carbon monoxide tolerance of the catalyst, thus promotes the performance noticeably.

3.3.2. Effect of methanol concentration

Methanol concentration is another crucial parameter which has a significant importance on the performance of DMFCs [51,52]. The experiments therefore were repeated at the operating temperatures that yield highest performance (80°C for MEA-1 and 100°C for MEA-2 and MEA-3) with the methanol concentrations of 0.75 M and 1.50 M to investigate the effect of the methanol concentration on the performances of the MEAs. The power density and polarization curves obtained from these experiments are shown in Fig.8. As seen from Fig.8(a), the peak power densities at 0.75 M and 1.50 M for MEA-1 were found as 518.52 W/m² and 418.68 W/m², respectively. In addition, the maximum power density (537.48 W/m²) of this MEA was achieved at 80°C and 1.00 M methanol concentration. As previously mentioned, however, the most appropriate operating temperature that gives the highest performance for MEA-2 and MEA-3 was found as 100°C. Therefore, the experiments were carried out at this temperature varying the methanol concentration from 0.75 M to 1.50 M. As seen from Figs.8(b) and (c), the peak power densities of MEA-2 and MEA-3 at the methanol concentrations of 0.75 M were found as 485.40 W/m² and 419.04 W/m², respectively. As the methanol concentration increases from 0.75 M to 1.50 M, the power densities of MEA-2 and MEA-3 decrease from 485.40 W/m² to 441.72 W/m² and 419.04 W/m² to 312.12 W/m², respectively. In addition, the maximum power densities of MEA-2 and MEA-3 were found as 551.52 W/m² and 445.44 W/m², respectively, when the methanol was supplied with the concentration of 1.00 M.

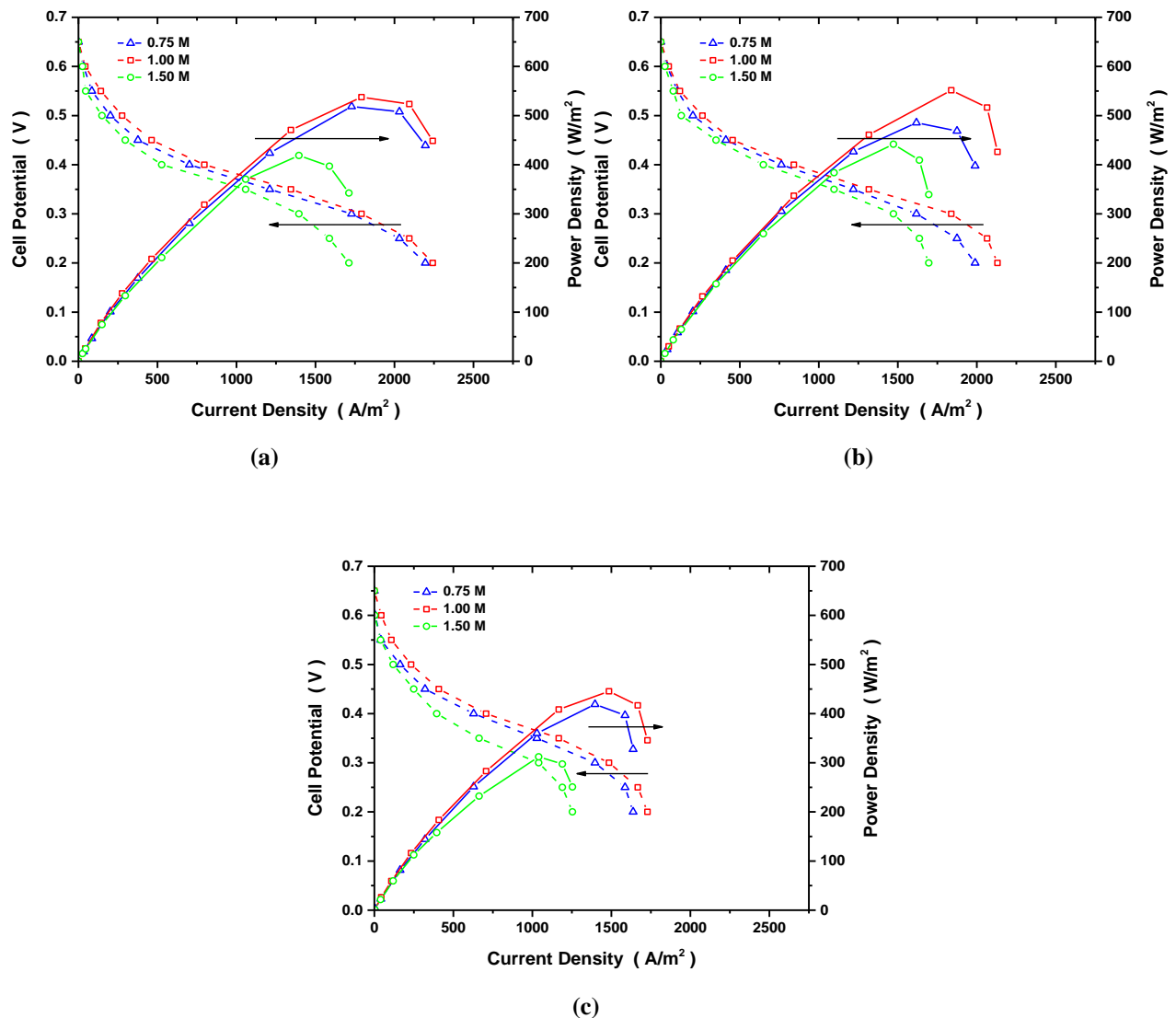


Fig.8. Power density and polarization curves at the methanol concentrations of 0.75 M, 1.00 M, and 1.50 M for (a) MEA-1 at 80°C, (b) MEA-2 at 100°C, and (c) MEA-3 at 100°C.

As presented in Figs.8(a)-(c), methanol concentration affects the performance of each DMFC considerably. This is because the concentration of methanol supplied to DMFC has a significant effect on the mass transport rate of methanol to the backing layers and the rate of methanol crossover from the anode to cathode. If the methanol with the optimum concentration is supplied to DMFC, it could be possible to achieve an improved DMFC performance. When the cell is fed with relatively low methanol concentrations, the OCV value becomes higher, whereas the limiting current density becomes lower because of the mass transport limitations. As the methanol concentration is increased from 1.00 M to 1.50 M, the cell voltage at low current densities becomes very low due to the significant increase in the rate of methanol crossover. The crossed-over methanol at the cathode is generally oxidized by the cathode catalyst, and thus leads to a mixed potential and undeniable voltage drop. Because of this methanol crossover problem, both the oxygen consumption and water generation rates within the cathode catalyst increase. The accumulated water causes a considerable increase in the mass transfer resistance within the cathode backing and catalyst layers. This would further decrease the available oxygen at the catalyst layer. These effects would, in the end, increase the cathodic activation and concentration polarizations. Due to the previously discussed negative effects of the methanol crossover problem, the achieved power densities become less after a certain methanol concentration value, which corresponds to ~1.00 M. As can be seen from Figs.8(a)-(c), with a further increase in the methanol concentration, the drop in the performance of MEA-1

becomes much more significant as compared to those of MEA-2 and MEA-3. This could be explained by the fact that with an increase in the methanol concentration, Nafion® 115 membrane loses its ability to remain physically stable, and the methanol crossover phenomenon becomes much more drastic. This results in a remarkable performance deterioration due to crossed-over methanol at the cathode. However, Nafion/ZrP composite membranes could remain physically stable and limit the methanol crossover in comparison to Nafion® 115 with the increase in the methanol concentration.

3.3.3. Effect of incorporation of ZrP into Pt/C cathode catalyst

ZrP is a solid proton conductor and provides solid state ion conductivity and high chemical and thermal stability [53]. Therefore, addition of ZrP directly to the commercial Pt/C cathode catalyst may improve the proton conductivity, reinforce the chemical and thermal stability, and allow operating at higher temperatures for DMFCs. In order to investigate the effect of Pt/C-ZrP cathode catalyst on the performance of the DMFCs, two different MEAs having the same NZ-2.5 but different cathode catalysts were manufactured. Then, to investigate the effect of operating temperature on the performances of these MEAs and make performance comparison, the experiments were conducted at different operating temperatures (40°C, 60°C, 80°C, and 100°C) and the methanol concentration of 1.00 M. Fig.9 presents the results of the experiments conducted for investigating the effect of operating temperature. As seen from Fig.9(a), the peak power densities at 40°C, 60°C, 80°C (for 1.00 M methanol concentration) were achieved as 243.72 W/m², 361.44 W/m², and 517.44 W/m² for MEA-4, respectively. In addition, the maximum power density was found as 591.02 W/m² at 100°C and 1.00 M. The same experiments were also conducted at the same operating temperatures and the methanol concentration of 1.00 M for MEA-5. As seen from Fig.9(b), the peak power densities at 40°C, 60°C, 80°C and 1.00 M were found as 280.20 W/m², 388.92 W/m², 561.84 W/m², respectively. The maximum power density was achieved as 620.88 W/m² at 100°C and 1.00 M. The potential reason of performance improvement with increasing operating temperature could be explained by the same mechanisms as discussed in Section 3.3.1. It is also found that MEA-5 yielded 5.06% more peak power density as compared to MEA-4. This performance improvement could be explained by the positive effects of incorporation of ZrP into commercial Pt/C cathode catalyst: higher and stable solid-state ion conductivity and better thermal and chemical stability.

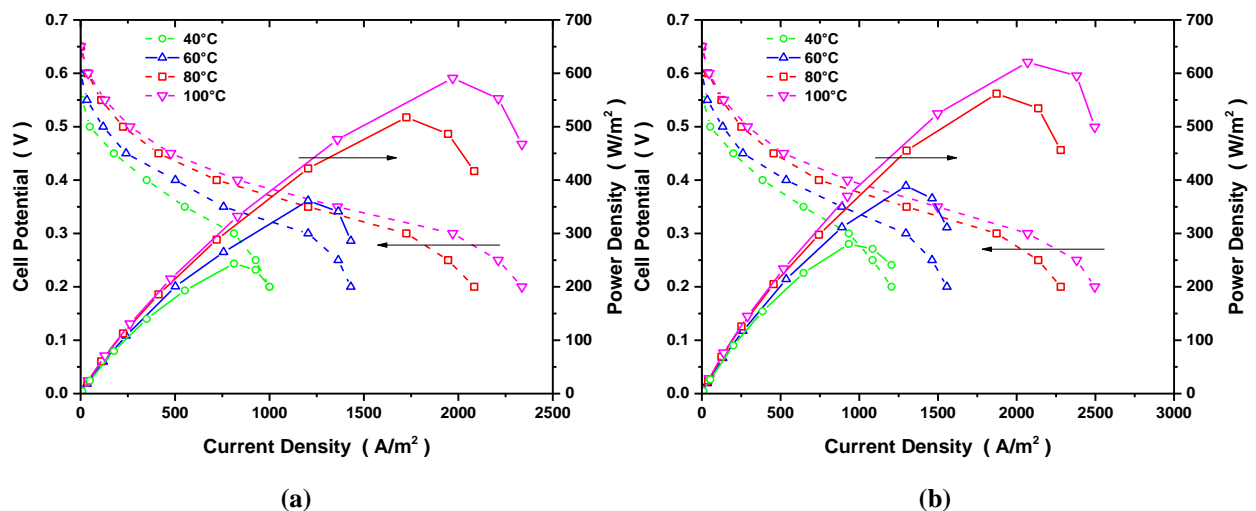


Fig.9. Power density and polarization curves at 40°C, 60°C, 80°C, 100°C and 1.00 M methanol concentration for (a) MEA-4, (b) MEA-5.

As reported above, the maximum performances of the MEAs were achieved at 100°C. Then, the experiments were carried out at different methanol concentrations (0.75 M and 1.50 M) and this operating temperature to investigate the effect of methanol concentration on the DMFC performance. As presented in Fig.10(a), the maximum power density was found as 591.02 W/m² for MEA-4 at 1.00 M and 100°C. As seen from Fig.10(b), the similar trend was also performed by MEA-5 with the maximum power density value of 620.88 W/m² at 1.00 M and 100°C. These trends in the performance variation with different methanol concentration were similar to

those discussed in Section 3.3.2. Therefore, the performance variation with the change in methanol concentration could be explained by the same mechanisms as discussed in Section 3.3.2. On the other hand, as the concentration of the methanol was increased from 1.00 M to 1.50 M, the achieved peak power densities demonstrated a noticeable decrease (18.8% and 16.5%) for MEA-4 and MEA-5, respectively. The observed performance deterioration for MEA-5 was relatively low and this could be associated with the improved chemical stability and proton conductivity of this MEA due to the incorporation of ZrP.

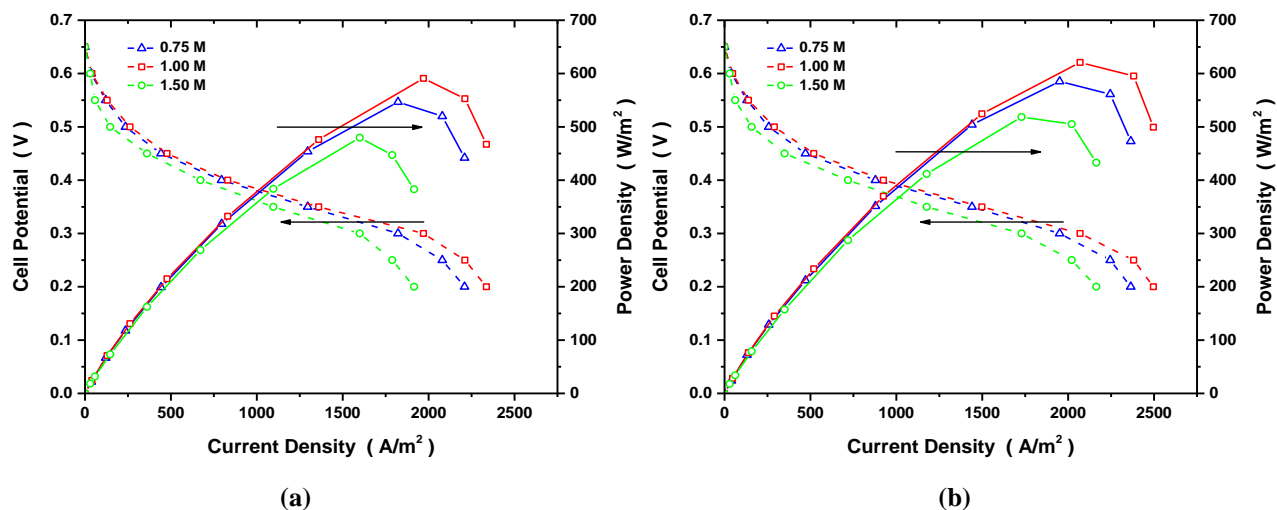


Fig.10. Power density and polarization curves at 0.75 M, 1.00 M, and 1.50 M and 100°C for (a) MEA-4, (b) MEA-5.

3.3.4. Stability tests

In addition to the polarization curve, the stability of MEA is an important factor for evaluating its suitability. In this regard, it is desired for a fuel cell that the power density drop with time is minimum [54]. Therefore, the short-term stability tests were carried out for all the MEAs to investigate their stability characteristics. During the stability tests, the flow rates of the 1.00 M methanol solution and oxygen gas were kept at 1.94 ml/min and 200 ml/min, respectively. The cell temperature and the voltage were set to 80°C and 0.3 V, respectively. The power density values were recorded for 4 h as seen in Fig.11. This figure shows that the majority of power density loss occurred in the first 15 minutes due to the instability of testing. In addition, a slow drop in the power densities of the MEAs associated with increasing amount of methanol at the cathode due to undesired methanol crossover was observed. Therefore, the presented stability characteristics in Fig.11 could also give a hint of each MEA's ability to mitigate this performance-limiting phenomenon. On the other hand, sudden drops and increases in the power densities were also observed due mainly to some occasional situations during the short-term stability tests. As seen from Fig.11, after 3 h operation at above-mentioned conditions, MEA-1, MEA-2, and MEA-3 started to provide less power densities at 0.3 V; however, the drops in the power densities of MEA-2 and MEA-3 much more than that of MEA-1 (Fig.11). These differences could be an indicator of the superiority of Nafion® 115 membrane over both NZ-2.5 and NZ-5 as regards stability. However, as seen from Fig.11, the drop in the power density of MEA-3 at 0.3 V is much more observable than that of MEA-2; therefore, the stability characteristic of NZ-2.5 is considered to be more promising in comparison to NZ-5. Fig.11 also clearly indicates that MEA-4 exhibits better stability characteristics as compared to MEA-2. This behavior could be attributed to the superiority of the HiSPEC® 9100 over commercial HP cathode catalyst (60 wt.% Pt on Vulcan XC-72) in terms of stability. Finally, as seen from Fig.11, incorporation of ZrP into commercial (HiSPEC® 9100) cathode catalyst could be the main reason for the MEA-5 demonstrating much better stability as compared to MEA-4.

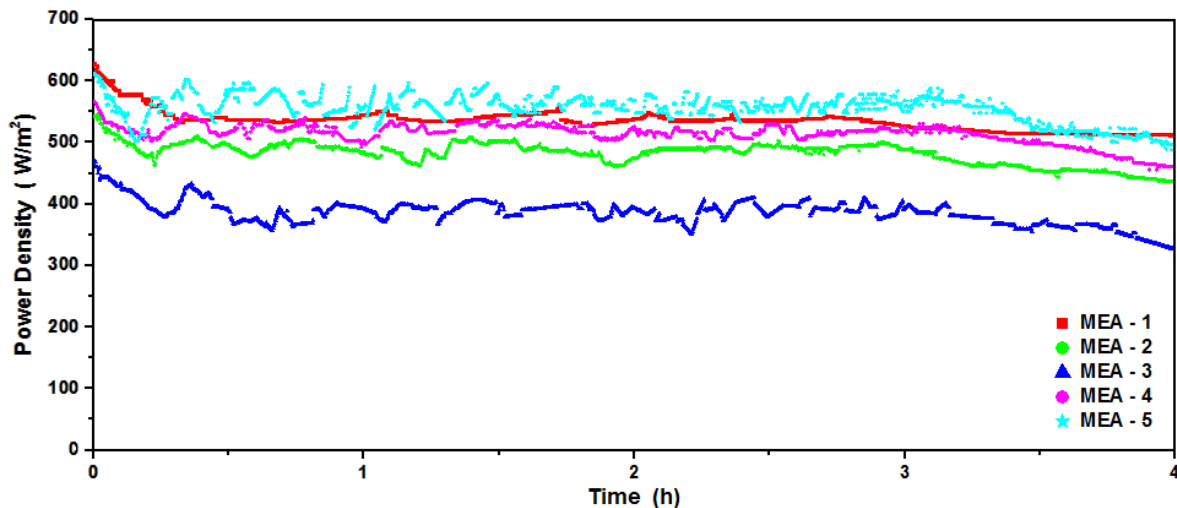


Fig.11. Short-term stability characteristics of the MEAs.

4. Conclusions

In this study, the performances of the MEAs having commercial Nafion[®] 115 membrane and NZ-2.5 and NZ-5 were investigated experimentally. The experiments were first performed at different temperatures (40°C, 60°C, 80°C, and 100°C) with the methanol concentration of 1.00 M to determine the temperatures, which each MEA yields its highest power density value. These temperature values were found as 80°C and 100°C for the MEAs having commercial Nafion[®] 115 membrane and Nafion/ZrP composite membranes, respectively. Then, a set of experiments were conducted at these temperatures with three different methanol concentrations (0.75 M, 1.00 M, and 1.50 M) to assess how the performances of the MEAs change depending on the methanol concentration. In addition, the performance of the MEA based on Pt/C-ZrP cathode catalyst and Nafion/ZrP composite membrane was compared with that of the MEA based on the same membrane but the conventional Pt/C cathode catalyst. In addition, short-term stability tests were carried out for all the MEAs. The main conclusions derived from the conducted study are listed as follows.

- The maximum power density of the MEA with commercial Nafion[®] 115 membrane was achieved at 80°C and 1.00 M methanol concentration with the power density value of 537.48 W/m².
- The MEA having NZ-2.5 provided its maximum power density (551.52 W/m²) at the temperature of 100°C and 1.00 M methanol concentration.
- The maximum power density provided by the MEA having NZ-5 was found as 445.44 W/m² at 100°C and 1.00 M methanol concentration.
- As the temperature increases 80°C to 100°C, the performance of the MEA having Nafion[®] 115 membrane deteriorates, whereas those of the MEAs having Nafion/ZrP composite membranes improve.
- For all the studied operating temperatures (40°C, 60°C, 80°C, and 100°C), the maximum power density (551.52 W/m²) was provided by the MEA having NZ-2.5 at 100°C.
- For all the studied methanol concentrations (0.75 M, 1.00 M, and 1.50 M), all the MEAs manufactured in this study provided their maximum power density values at 1.00 M methanol concentration.
- The MEA having commercial Nafion[®] 115 membrane shows more promising behavior regarding stability as compared to the MEAs having NZ-2.5 and NZ-5.
- Introduction of ZrP to commercial (HiSPEC[®] 9100) cathode catalyst improves both the performance and the stability characteristic of the MEA.
- The MEA with NZ-2.5 and commercial (HiSPEC[®] 9100) cathode catalyst seems more promising in terms of both performance and stability as compared to the MEA having the same membrane but commercial (HP 60 wt.% Pt on Vulcan XC-72) cathode catalyst.

The results of this study have revealed that the MEA having NZ-2.5 provides distinguishably better performance in comparison to the MEA with commercial Nafion® 115 membrane at elevated operating temperatures. As a future study, long-term stability tests will be carried out to assess the suitability of these membranes for DMFC applications.

5. Acknowledgements

This project has received funding from the European Union's Horizon 2020 research and innovation programme under the Marie Skłodowska-Curie grant agreement No 661579. The authors would also like to acknowledge the technical support of TEKSIS (a company located in the technology development zone of Middle East Technical University campus in Ankara, Turkey) in the setup and calibration of the DMFC test station.

References

- [1] Schonert M, Jakoby K, Schlumbohm C, Glüsen A., Mergel J, Stolten D. Manufacture of robust catalyst layers for the DMFC. *Fuel Cells* 2004;4:175–9. doi:10.1002/face.200400027.
- [2] Liu H, Song C, Zhang L, Zhang J, Wang H, Wilkinson DP. A review of anode catalysis in the direct methanol fuel cell. *Journal of Power Sources* 2006;155:95–110. doi:10.1016/j.jpowsour.2006.01.030.
- [3] Colpan CO, Cruickshank CA, Matida E, Hamdullahpur F. 1D modeling of a flowing electrolyte-direct methanol fuel cell. *Journal of Power Sources* 2011;196:3572–82. doi:10.1016/j.jpowsour.2010.12.013.
- [4] Yang B, Manthiram A. Sulfonated Poly(ether ether ketone) Membranes for Direct Methanol Fuel Cells. *Electrochemical and Solid-State Letters* 2003;6:A229. doi:10.1149/1.1613073.
- [5] Wang S, Sun G, Wang G, Zhou Z, Zhao X, Sun H, Fan X, Yi B, Xin Q. Improvement of direct methanol fuel cell performance by modifying catalyst coated membrane structure. *Electrochemistry Communications* 2005;7:1007–12. doi:10.1016/j.elecom.2005.07.003.
- [6] Basri S, Kamarudin SK, Daud WRW, Yaakub Z. Nanocatalyst for direct methanol fuel cell (DMFC). *International Journal of Hydrogen Energy* 2010;35:7957–70. doi:10.1016/j.ijhydene.2010.05.111.
- [7] Mauritz KA, Moore RB. State of understanding of Nafion. *Chemical Reviews* 2004;104:4535–85. doi:10.1021/cr0207123.
- [8] Sridhar P, Perumal R, Rajalakshmi N, Raja M, Dhathathreyan KS. Humidification studies on polymer electrolyte membrane fuel cell. *Journal of Power Sources* 2001;101:72–8. doi:10.1016/S0378-7753(01)00625-5.
- [9] Ercelik M, Ozden A, Devrim Y, Colpan CO. Investigation of Nafion Based Membranes on the Performance of DMFCs. *International Journal of Hydrogen Energy*, Corrected Proof, Available online, 18 July 2016, In press, doi: 10.1016/j.ijhydene.2016.06.215.
- [10] Devrim Y, Erkan S, Baç N, Eroglu I. Improvement of PEMFC performance with Nafion/inorganic nanocomposite membrane electrode assembly prepared by ultrasonic coating technique. *International Journal of Hydrogen Energy* 2012;37:16748–58. doi:10.1016/j.ijhydene.2012.02.148.
- [11] Rosenthal NS, Vilekar SA, Datta R. A comprehensive yet comprehensible analytical model for the direct methanol fuel cell. *Journal of Power Sources* 2012;206:129–43. doi:10.1016/j.jpowsour.2012.01.080.
- [12] Wu J, Yuan XZ, Martin JJ, Wang H, Zhang J, Shen J, Wu S, Merida W. A review of PEM fuel cell durability: Degradation mechanisms and mitigation strategies. *Journal of Power Sources* 2008;184:104–19. doi:10.1016/j.jpowsour.2008.06.006.
- [13] Yang C, Costamagna P, Srinivasan S, Benziger J, Bocarsly AB. Approaches and technical challenges to high temperature operation of proton exchange membrane fuel cells 2001;103:1–9.

- [14] Wannek C, Glüsen A, Stolten D. Materials, manufacturing technology and costs of fuel cell membranes. *Desalination* 2010;250:1038–41. doi:10.1016/j.desal.2009.09.102.
- [15] Staiti P, Aricò A, Baglio V, Lufrano F, Passalacqua E, Antonucci V. Hybrid Nafion–silica membranes doped with heteropolyacids for application in direct methanol fuel cells. *Solid State Ionics* 2001;145:101–7. doi:10.1016/S0167-2738(01)00919-5.
- [16] Chalkova E, Fedkin MV, Wesolowski DJ, Lvov SN. Effect of TiO₂ Surface Properties on Performance of Nafion-Based Composite Membranes in High Temperature and Low Relative Humidity PEM Fuel Cells. *Journal of The Electrochemical Society* 2005;152:A1742. doi:10.1149/1.1971216.
- [17] Jalani NH, Dunn K, Datta R. Synthesis and characterization of Nafion[®]-MO₂ (M = Zr, Si, Ti) nanocomposite membranes for higher temperature PEM fuel cells. *Electrochimica Acta* 2005;51:553–60. doi:10.1016/j.electacta.2005.05.016.
- [18] Yu TL, Lin H-L, Shen K-S, Huang L-N, Chang Y-C, Jung G-B, Huang J-C. Nafion/PTFE Composite Membranes for Fuel Cell Applications. *Journal of Polymer Research* 2004;11:217–24. doi:10.1023/B:JPOL.0000043408.24885.c6.
- [19] Lin H-L, Yu TL, Huang L-N, Chen L-C, Shen K-S, Jung G-B. Nafion/PTFE composite membranes for direct methanol fuel cell applications. *Journal of Power Sources* 2005;150:11–9. doi:10.1016/j.jpowsour.2005.02.016.
- [20] Chen L-C, Yu TL, Lin H-L, Yeh S-H. Nafion/PTFE and zirconium phosphate modified Nafion/PTFE composite membranes for direct methanol fuel cells. *Journal of Membrane Science* 2008;307:10–20. doi:10.1016/j.memsci.2007.03.008.
- [21] Molla S, Compan V. Performance of composite Nafion/PVA membranes for direct methanol fuel cells. *Journal of Power Sources* 2011;196:2699–708. doi:10.1016/j.jpowsour.2010.11.022.
- [22] Park Y, Kim J, Nagai M. Increase of proton conductivity in amorphous phosphate – Nafion membranes. *Journal of Materials Science Letters* 2000; 1621–3. doi: 10.1023/A:1006749706972.
- [23] Costamagna P, Yang C, Bocarsly AB, Srinivasan S. Nafion[®] 115/zirconium phosphate composite membranes for operation of PEMFCs above 100°C. *Electrochimica Acta* 2002;47:1023–33. doi:10.1016/S0013-4686(01)00829-5.
- [24] Shukla AK, Raman RK. Methanol-Resistant Oxygen-Reduction Catalysts For Direct Methanol Fuel Cells. *Annual Review of Materials Research* 2003;33:155–68. doi:10.1146/annurev.immunol.21.120601.141107.
- [25] Wang H, Xu C, Cheng F, Zhang M, Wang S, Jiang SP. Pd/Pt core-shell nanowire arrays as highly effective electrocatalysts for methanol electrooxidation in direct methanol fuel cells. *Electrochemistry Communications* 2008;10:1575–8. doi:10.1016/j.elecom.2008.08.011.
- [26] Antolini E, Salgado JRC, Gonzalez ER. The stability of Pt-M (M = first row transition metal) alloy catalysts and its effect on the activity in low temperature fuel cells. A literature review and tests on a Pt-Co catalyst. *Journal of Power Sources* 2006;160:957–68. doi:10.1016/j.jpowsour.2006.03.006.
- [27] Xu JB, Zhao TS, Yang WW, Shen SY. Effect of surface composition of Pt-Au alloy cathode catalyst on the performance of direct methanol fuel cells. *International Journal of Hydrogen Energy* 2010;35:8699–706. doi:10.1016/j.ijhydene.2010.05.008.
- [28] Selvarani G, Selvaganesh SV, Krishnamurthy S, Kiruthika GVM, Dhar S, Pitchumani S, Shukla AK. A methanol-tolerant carbon-supported Pt-Au alloy cathode catalyst for direct methanol fuel cells and its evaluation by DFT. *Journal of Physical Chemistry C* 2009;113:7461–8. doi:10.1021/jp810970d.
- [29] Alberti G, Casciola M, Costantino U, Levi G, Ricciardi G. On the mechanism of diffusion and ionic transport in crystalline insoluble acid salts of tetravalent metals-I Electrical conductance of zirconium bis (monohydrogen ortho-phosphate) monohydrate with a layered structure. *Journal of Inorganic and Nuclear Chemistry* 1978;40:533–7. doi:10.1016/0022-1902(78)80437-0.
- [30] Barron O, Su H, Linkov V, Pollet BG, Pasupathi S. Enhanced performance and stability of high

- temperature proton exchange membrane fuel cell by incorporating zirconium hydrogen phosphate in catalyst layer. *Journal of Power Sources* 2015;278:718–24. doi:10.1016/j.jpowsour.2014.12.139.
- [31] Xie Z, Navessin T, Shi Z, Chow R, Holdcroft S. Gas diffusion electrodes containing ZHP/Nafion for PEMFC operation at 120°C. *Journal of Electroanalytical Chemistry* 2006;596:38–46. doi:10.1016/j.jelechem.2006.06.018.
- [32] Kim BC, Spinks GM, Too CO, Wallace GG, Bae YH, Ogata N. Incorporation of novel polyelectrolyte dopants into conducting polymers. *Reactive and Functional Polymers* 2000;44:245–58. doi:10.1016/S1381-5148(99)00100-5.
- [33] Park YS, Yamazaki Y. High proton conducting and low methanol crossover Nafion/Hydroxyapatite (HA) composite membrane 2004.
- [34] Lim C, Wang CY. Development of high-power electrodes for a liquid-feed direct methanol fuel cell. *Journal of Power Sources* 2003;113:145–50. doi:10.1016/S0378-7753(02)00541-4.
- [35] Chen R, Zhao TS, Liu JG. Effect of cell orientation on the performance of passive direct methanol fuel cells. *Journal of Power Sources* 2006;157:351–7. doi:10.1016/j.jpowsour.2005.07.073
- [36] Alfa Aesar. User Instructions for DMFC Electrodes & MEAs Prior to Installation.
- [37] Barbora L, Acharya S, Verma A. Synthesis and ex-situ characterization of Nafion/TiO₂ composite membranes for direct ethanol fuel cell. *Macromolecular Symposia* 2009;277:177–89. doi:10.1002/masy.200950322.
- [38] Devrim Y. Preparation and testing of Nafion/titanium dioxide nanocomposite membrane electrode assembly by ultrasonic coating technique. *Journal of Applied Polymer Science* 2014;131:15. doi:10.1002/app.40541.
- [39] Kuan H-C, Wu C-S, Chen C-Y, Yu Z-Z, Dasari A, Mai Y-W. Preparation of Exfoliated Zirconium Phosphate/Nafion Organic-Inorganic Hybrid Proton Exchange Membranes. *Electrochemical and Solid-State Letters* 2006;9:A76–9. doi:10.1149/1.2149207.
- [40] Mokhtaruddin SR, Mohamad AB, Shyuan LK, Kadhum AAH, Akhmad M. Preparation and Characterization of Nafion-Zirconia Composite Membrane for PEMFC. *Advanced Materials Research* 2011;239-242:263–8. doi:10.4028/www.scientific.net/AMR.239-242.263.
- [41] Bauer F, Willert-Porada M. Microstructural characterization of Zr-phosphate-Nafion[®] membranes for direct methanol fuel cell (DMFC) applications. *Journal of Membrane Science* 2004;233:141–9. doi:10.1016/j.memsci.2004.01.010.
- [42] Rodgers MP, Shi Z, Holdcroft S. Ex situ characterisation of composite nafion membranes containing zirconium hydrogen phosphate. *Fuel Cells* 2009;9:534–46. doi:10.1002/face.200900027.
- [43] He R, Li Q, Xiao G, Bjerrum NJ. Proton conductivity of phosphoric acid doped polybenzimidazole and its composites with inorganic proton conductors. *Journal of Membrane Science* 2003;226:169–84. doi:10.1016/j.memsci.2003.09.002.
- [44] Tripathi BP, Shahi VK. SPEEK-zirconium hydrogen phosphate composite membranes with low methanol permeability prepared by electro-migration and in situ precipitation. *Journal of Colloid and Interface Science* 2007;316:612–21. doi:10.1016/j.jcis.2007.08.038.
- [45] Devrim, Y. Fabrication and performance evaluation of hybrid membrane based on a sulfonated polyphenyl sulfone/phosphotungstic acid/silica for proton exchange membrane fuel cell at low humidity conditions. *Electrochimica Acta* 2014; 146, 741-751. doi:10.1016/j.electacta.2014.08.131.
- [46] Shao Z-G, Joghee P, Hsing I-M. Preparation and characterization of hybrid Nafion–silica membrane doped with phosphotungstic acid for high temperature operation of proton exchange membrane fuel cells. *Journal of Membrane Science* 2004;229:43–51. doi:10.1016/j.memsci.2003.09.014.
- [47] Singha S, Jana T. Structure and Properties of Polybenzimidazole/Silica Nanocomposite Electrolyte Membrane: Influence of Organic/Inorganic Interface. *ACS Applied Materials & Interfaces* 2014;6:21286–96. doi:10.1021/am506260j.
- [48] Liu H, Zhang J. *Electrocatalysis of Direct Methanol Fuel Cells: From fundamentals to applications*. Wiley-Vch 2009. doi:10.1002/9783527627707.
- [49] Heinzel A., Barragan VM. Review of the state-of-the-art of the methanol crossover in direct methanol fuel cells. *Journal of Power Sources* 1999;84:70–4. doi:10.1016/S0378-7753(99)00302-X.
- [50] Bauer F, Willert-Porada M. Comparison between Nafion[®] and a Nafion[®] zirconium phosphate nano-

- composite in fuel cell applications. *Fuel Cells* 2006;6:261–9. doi:10.1002/fuce.200500217.
- [51] Ravikumar MK, Shukla AK. Effect of Methanol Crossover in a Liquid Feed Polymer Electrolyte Direct Methanol Fuel Cell. *Journal of The Electrochemical Society* 1996;143:2601–6. doi:10.1149/1.1837054.
- [52] Ozden A, Ercelik M, Ouellette D, Colpan CO, Ganjehsarabi H, Hamdullahpur F. Designing, modeling and performance investigation of bio-inspired flow field based DMFCs. *International Journal of Hydrogen Energy*, Corrected Proof, Available online, 23 January 2017, In press, doi: 10.1016/j.ijhydene.2017.01.007.
- [53] Jiang R, Russell Kunz H, Fenton JM. Influence of temperature and relative humidity on performance and CO tolerance of PEM fuel cells with Nafion®-Teflon®-Zr(HPO₄)₂ higher temperature composite membranes. *Electrochimica Acta* 2006;51:5596–605. doi:10.1016/j.electacta.2006.02.033.
- [54] Ercelik M, Ozden A, Seker E, Colpan CO. Characterization and performance evaluation of Pt-Ru/C-TiO₂ anode electrocatalyst for DMFC applications. *International Journal of Hydrogen Energy*, Corrected Proof, Available online, 26 December 2016, In press, doi: 10.1016/j.ijhydene.2016.12.020.